Article:
Whittle, J.W., Danks, S., Koh, L.S.C. et al. (2026) Quantifying the influence of sleeper spacing on lateral resistance using a novel experimental method. Railway Engineering Science. ISSN: 2662-4745

https://doi.org/10.1007/s40534-026-00430-x

Railway Engineering Science
https://doi.org/10.1007/s40534-026-00430-x

Quantifying the influence of sleeper spacing on lateral resistance using a novel experimental method

Jacob W. Whittle[1] · **Stephen Danks**[2] · **Lenny S. C. Koh**[3] · **David I. Fletcher**[1]

Received: 8 August 2025 / Revised: 8 January 2026 / Accepted: 15 January 2026

Abstract
Lateral resistance, principally dictated by the interaction between sleepers (ties) and ballast, is a fundamental property of ballasted railway track which is critical to overall track stability and safety. This study investigates the influence of sleeper spacing on lateral resistance to support overall track system design and track safety management. A novel multi-sleeper push test (MSPT) methodology, utilising both a kinematic restraint to better replicate track conditions and a state-of-the-art digital image correlation (DIC) system to measure surface ballast movement, has been used to evaluate the lateral resistance behaviour of two different sleeper types (concrete and steel) under seven different sleeper spacing conditions (550–850 mm). This is the first direct comparison of modern concrete and steel sleeper variants under these conditions. It is found that both sleeper types exhibit similar lateral resistance behaviour at small displacements (less than 3 mm) but, regardless of the spacing used, steel sleepers have significantly greater lateral resistance beyond this point. Although it depends on the assessment method used, concrete sleepers demonstrated an optimum spacing of approximately 675 mm, whilst steel sleepers showed highest resistance at approximately 706 mm. However, concrete sleepers showed less sensitivity to changes in spacing compared to steel sleepers, which retained high resistance over a narrower range of spacings. These findings contribute to track safety management by improving buckling mitigation strategies and component selection, whilst unlocking the ability to assess system-level impacts to aid the pursuit of more sustainable railway infrastructure design.

Keywords Sleeper · Ballast · Lateral resistance · Multi-sleeper push test · Railway track

1 Introduction

The railway track system is principally constructed from rails, sleepers (ties), and ballast [1]. The key function of railway sleepers is to transfer and distribute the loads arising from the wheel–rail contact to the ballast via the rails, transversely secure the rails to maintain the correct gauge width, and resist the abrading actions of ballast material [2, 3], thus providing stability to the rails and enabling the system to resist lateral movement [4, 5]. A core feature of modern railway track is railway sleeper spacing which is periodic (i.e. regularly spaced). The definition of this separation distance is important as it, in turn, influences the response of the overall track system [6–8]. Consequently, effective and accurate characterisation of the track system, and the parameters which affect it, is vital to wider vehicle–track interaction studies [9]. For example, spacing can influence the vibration and resonance at the wheel–rail contact [10] which can cause accelerated track damage (e.g. rail wear, rail corrugation) leading to degradation in track performance and overall life [11–14]. Current global track system design standards suggest, under a first order analysis, that the lateral resistance of ballast is expected to remain constant throughout the normal range of sleeper spacing (see below) [15–17]. However, this neglects an important second order effect in which a change in sleeper spacing alters the amount of ballast which interacts between each adjacent sleeper, known as the 'zone of influence' [7]. As shown in Fig. 1, this behaviour can significantly affect the amount of ballast moved by the track system.

✉ Jacob W. Whittle
jwwhittle1@sheffield.ac.uk

[1] School of Mechanical, Aerospace, and Civil Engineering, University of Sheffield, Sheffield S1 3JD, UK

[2] British Steel, Brigg Road, Scunthorpe, North Lincolnshire DN16 1XA, UK

[3] Management School, University of Sheffield, Sheffield S10 1FL, UK

Published online: 27 February 2026

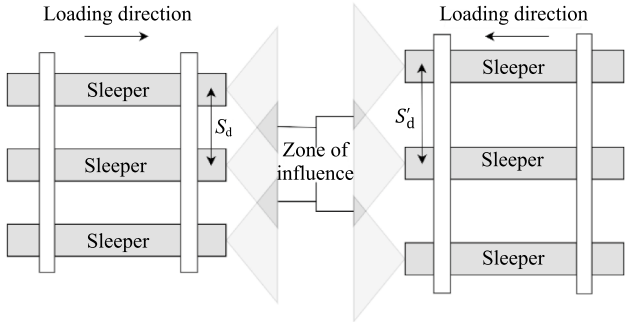

Fig. 1 Influence of sleeper spacing on lateral resistance, adapted from [7]

Sleeper spacing has organically evolved over time and is dictated by a number of operational factors including vehicle and axle speed, track layout, and track dynamic effects in an attempt to minimise issues at the wheel–rail contact and overall track structure [9, 18, 19]. Globally, sleeper spacing values typically fall within 550 – 850 mm across a range of sleeper types and specifications including timber, concrete, steel, and composite. Although, some countries (including Italy, Nepal, and Canada) have examples of spacings greater (e.g. 900 mm) and smaller (e.g. 495 mm) than the typical range [9]; these generally arise from specific infrastructure requirements (e.g. mining operations). There can be significant economic and environmental benefits to increasing sleeper spacing due to the reduced number of components procured and installed. However, many of these separation distances have roots in historical trial and error. This means they have not been formally optimised, potentially resulting in sub-optimal installation cost, life environmental impact, and maintenance cost. Therefore, this paper reports the importance of sleeper spacing with respect to lateral resistance in ballasted track, applying recently developed test [20] and visualisation [21] methods modified for this purpose. Although it is recognised that changes in spacing could have other positive (e.g. a reduction in environmental impact) and negative (e.g. an increase in track stiffness) impacts on track system, these are not the core focus of this study.

1.1 Lateral resistance

Lateral resistance, principally dictated by the sleeper–ballast interaction, is a property of ballasted railway track critical to overall track stability, and ultimately reducing track buckling risk [4, 5, 22]. The resistance available at the interface between sleeper and ballast can be characterised by a force–displacement curve, which typically consists of a rapid rise in force followed by a near constant plateau after a short lateral displacement (usually less than 5 mm) [21]. This property is called lateral resistance (R_t) and can be considered as the sum of the three components acting on the bottom (R_b), side (R_s), and end (R_e) of the sleeper. The R_b and R_s components are a result of frictional forces of the ballast against the sleeper as it moves, while the end force (R_e) results from reaction forces of the ballast on the sleeper end

Table 1 Summary of MSPT lateral resistance studies

Author, Year	Sleeper type	Test method (closest standard)	Sleeper spacing (mm)	Disp. value	Ballast condition	Bed condition	Lateral resistance (kN/sleeper)	Lateral resistance (kN/m)
De Iorio et al., 2014 [36]	Concrete RFI230 (EG47 equivalent)	Field MSPT (4 sleepers) †1	600	Peak (kN)	U	FCFS	5.55	Not reported
	Concrete RFI240 (G44 equivalent)				U		7.72	
					DTS C		8.84	
De Iorio et al., 2018 [34]	Concrete FSV35P (EG47 equivalent)	Field MSPT (4 sleepers) †2	600	Peak (kN)	DTS C	FCFS	5.88	9.80
					DTS C	NCNS	1.60	2.67
Pucilio, 2020 [37]	Concrete RFI240 (G44 equivalent)	Field MSPT †2	600	Peak (kN)	U	FCFS	6.87	Not reported
		Field MSPT †2			C		8.34	
Pucilio et al., 2018 [38]	Concrete RFI240 (G44 equivalent)	Field MSPT (4 sleepers) †2	600	Peak (kN)	Trafficked C	FCFS	6.87	Not reported
					DTS C		7.95	
Reiner, 1977 [39]	Concrete RT7	Field MSPT (39 ft) †2	508	47.75 mm	Tamped C	FCFS	3.53	Not reported
				46.74 mm	C		4.68	
	Timber			41.66 mm	Tamped C		2.63	
				18.81 mm	C		2.88	
Van't Zand and Moraal, 1997 [40]	Concrete NS90 (G44 equivalent)	Laboratory MSPT (5 sleepers) †2	Not noted	Peak (kN)	Tamped C	FCHS	9.00	Not reported

DTS dynamic track stabilisation, FC full crib, NC no crib, FS full shoulder, HS half shoulder, NS no shoulder, U unconsolidated, C consolidated, †1 UIC field method and †2 own method

[23]. As noted in Fig. 1, the total lateral resistance generated by the track system can be affected by inter-sleeper–ballast interaction between neighbouring sleepers; but the extent of this contribution is unclear within previous research [24]. Lateral resistance can also be influenced by factors including ballast consolidation [25–28], ballast condition [29–31], ballast support [32], and ballast dimensions [33].

1.2 Lateral resistance test methods and values

Two core methods exist for testing lateral resistance within a laboratory, the single sleeper push test (SSPT) [33] and track panel push test (TPPT) [34], referred generically to here-in as a multi-sleeper push test (MSPT). There are a number of standardised test methods which incorporate elements of both types of test including UIC [35], SNCF [35], TUM [35], and BS500:2000 [25] but adoption varies widely between country, study, and environment. As reported in existing literature, very few studies undertake MSPTs, at full-scale, either in a laboratory environment, within a simulation environment, or in the field due to the perceived complexity of work compared to a SSPT [23], which also means very few elect to investigate the spacing parameter [9]. Previous studies are summarised in Table 1.

The studies noted in Table 1 account for approximately a quarter of all existing literature since 1970 which investigate lateral resistance behaviour and are the only examples of studies which include an assessment of the influence of sleeper spacing on lateral resistance behaviour through MSPTs. This review found that this is predominantly done through field experiments, with a single example of laboratory experiments. Surprisingly, this review found no open-literature studies employing computational simulations to investigate sleeper spacing effects. The variety of study goals, parameters, and test locations means that the way which a study is carried out is generally not standardised, beyond de facto lateral displacement distances dictated by physical constraints. This makes true comparison between studies difficult. However, most studies elect to study a complete ballast bed (i.e. full crib, full shoulder) under consolidated ballast conditions. Furthermore, within the collected literature on lateral resistance, as shown in Table 1, all but one study focuses on a single sleeper type with the outlier drawing a comparison between two types, while studies on sleeper failure and degradation across multiple types exist [41, 42], existing lateral resistance research focuses only on, either, timber or concrete sleeper variants at fixed sleeper spacings. This leaves a significant gap in accurately quantifying how alternative sleeper types (including steel and composite) behave under a range of sleeper spacings in near identical conditions. Even for tests with the same sleeper type and ballast condition, the resultant lateral resistance values reported can vary widely. However, there is much less variation in a MSPT test configuration compared to values reported by existing SSPT literature, indicating a methodology advantage. Finally, although lateral resistance values normalised per metre of track (kN/m) can be easily derived, only De Iorio et al. [34] elected to report values in this unit; likely due to most studies focusing only on a single fixed spacing.

A gap therefore exists in comparable evaluation of the effect of sleeper spacing on lateral resistance across multiple sleeper types. To address this physical testing has been conducted to quantify the lateral resistance behaviour of common railway sleepers; concrete (G44) and steel (W560H) at a range of sleeper spacings between 550 and 850 mm. The tests are performed only for consolidated ballast conditions, utilising a modified laboratory-based test method first developed by Słodczyk et al. [20]. The findings enhance understanding of lateral resistance performance characteristics of railway sleepers by qualitatively and quantitatively assessing behaviour, enabling the optimisation of spacing with respect to lateral resistance as well as forming inputs to wider vehicle–track interface models to help increase overall track performance.

This paper is structured as follows: Sect. 2 describes the study methodology, Sect. 3 presents the results and findings arising from the study, Sect. 4 discusses the results presented in Sect. 3, and Sect. 5 summarises key insights and their implications.

2 Methodology

2.1 Experimental apparatus

To achieve the aims of this paper, full-scale MSPT laboratory experiments were carried out in a ballast box. In this instance, three sleepers were used to construct the track panel as this is the fewest number which allows for the practical assessment of the sleeper spacing parameter. The box contained approximately 9 tonnes of ballast graded in accordance with Network Rail standard NR/L2/TRK/8100 [43]. The dimensions of the box, ballast, and shoulder can be seen schematically in Fig. 2. The ballast box is deliberately sized such that the widest sleeper spacing can be tested without the sides of the box influencing the lateral resistance generated [44].

The rail section at each end of the sleeper was fixed using the standard fasteners on each sleeper and was 2250 mm in length at each end to allow for maximum sleeper spacing adjustment. This sleeper test included the use of a kinematic vertical restraint made from two right angle steel sections of length several times that of the maximum push length secured to the frame (item 8), supporting the actuator (item 7). The contact distance between the rear rail load cells and

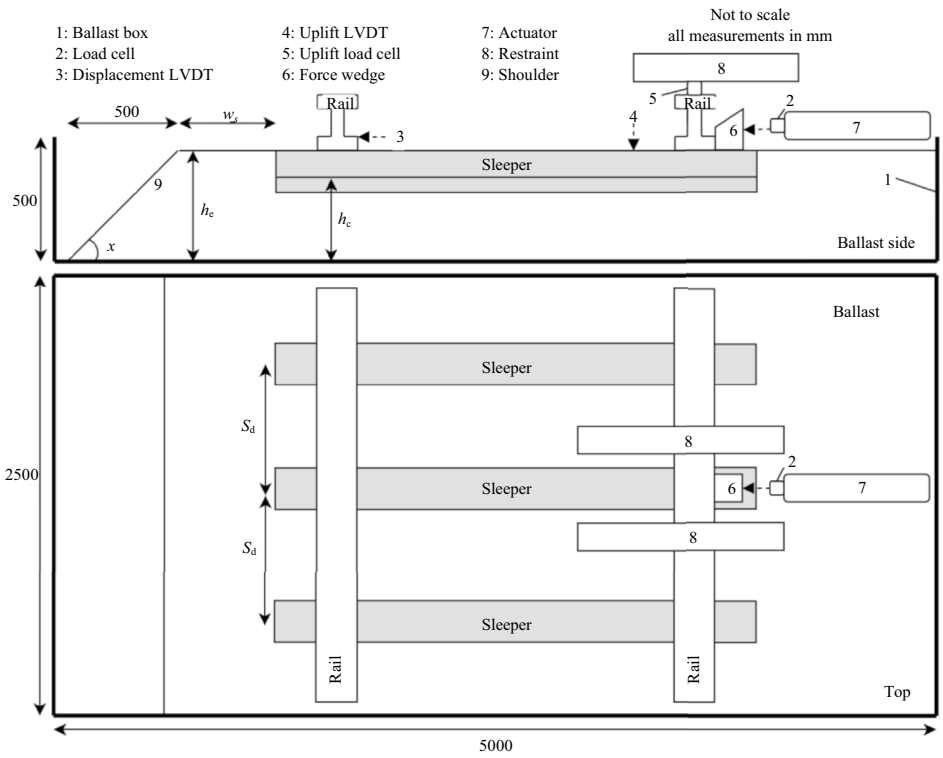

Fig. 2 Sleeper test rig schematic

restraint is minimised to near zero to limit the rotational moment applied to the sleeper arrangement, which also limits movement at the front of the sleeper panel [45].

As described by Słodczyk et al. [20], the effect of the rail resisting upwards movement of sleepers during lateral shift is achieved by the aforementioned steel sections remaining in constant contact throughout the test, thereby generating results which are more representative of in-service behaviour for all types of railway sleeper than existing methods [23]. Experimental testing, outlined in full within the Supplementary Information, has shown that this restraint is equivalent in vertical stiffness to that of a six-sleeper buckle, and that at small displacements is conservative in its restraint of vertical sleeper movement. When taken together, this suggests that results generated through use of the apparatus are generally conservative when compared to the real track system. This arrangement contrasts existing studies, in which a fixed, large (i.e. many times the weight of the panel) 'deadweight' is applied to the top of the sleeper panel to restrict vertical movement [40]. It is the view of the authors that neither this approach (i.e. effectively fixing the ability of the panel to lift) or one in which the sleepers can move freely, reflects how sleepers behave in track. In reality, a sleeper connected to the rail cannot rise freely because the rail provides some downward resistance. However, this resistance is limited because the rail and sleepers are not rigid and are generally not anchored to the ground. Therefore, the introduction of a restraint which can limit vertical movement, whilst not artificially restricting movement is an important methodological development.

It should be noted that the experimental configuration does not include additional active downward force on the sleeper (i.e. there is no representation of downward vehicle forces). While the vertical restraint helps maintain rail contact and supports lateral resistance measurements and has been shown to be conservative in its restraint of vertical sleeper movement when compared to a real track system, it may, as a result, unintentionally stop the formation of phenomena observed in the field (i.e. unsupported hanging sleepers) which can influence lateral resistance behaviour. Therefore, although likely conservative, the results generated from this apparatus should only be considered applicable to newly installed track that has not undergone repeated dynamic loading.

The lateral load was applied using a 60 kN linear actuator (item 7) which was placed at the end of the sleeper furthest from the ballast shoulder with its centreline 75 mm above the top face of the central sleeper to minimise the rotational moment applied to the sleeper panel. A ball and socket arrangement (item 6), not rigidly attached to the sleeper, was used as an interface between the actuator plate and the sleeper to transfer force through the fastener [20]. The

Fig. 3 Sleeper test experimental arrangement showing sleeper panel, ballast box (item 1), load cell (item 2), displacement LVDT (item 3), ball and socket load arrangement (item 6), restraint (item 8)

horizontal and vertical sleeper displacements were monitored directly by two linear variable differential transducers (LVDTs) (item 3 and item 4). The horizontal and vertical loads generated by the sleeper were measured by a 50 kN (item 2) and two 20 kN (item 5) load cells, respectively. A head on view of the experimental arrangement can be seen in Fig. 3.

Furthermore this ballast box is fitted with a bespoke digital image correlation (DIC) system, as described by Whittle et al. [21]. The system makes use of commodity camera equipment, positioned above the ballast box, and open-source algorithms to measure the movement of, primarily, ballast particles. This unlocks the ability to observe how ballast and sleepers interact, particularly ahead of and between adjacent sleepers.

2.2 Test procedure and program

Each sleeper type was tested under one ballast condition; consolidated (ballast density of approximately 1750 kgm^{-3}), one bed condition; full, and seven discrete sleeper spacings (s_d); 550 to 850 mm at 50 mm intervals. In order to create the full condition, the heights of h_c and h_e were formed coplanar to the top of the sleeper. The overall ballast layer thickness was approximately 380 mm. As shown in Fig. 2, the ballast shoulder angle (x) was set to approximately 45 degrees (the angle of material natural repose), with the shoulder width (w_s) set to 500 mm from the end of each sleeper (where shoulder and end both refer to all ballast beyond the end of the sleeper).

Each test was repeated three times with the complete program, including sleeper specification, summarised in Table 2. Each MSPT followed the procedure outlined by Słodczyk et al. [20] for test operation, modified to account for the installation of sleeper panel instead of a single sleeper, and Whittle et al. [21] for DIC image acquisition. In brief, each sleeper panel was installed into the ballast box and ballast added, formed, and consolidated. The panel was then displaced at a constant rate of 10 mm/min to a maximum lateral displacement of 40 mm, with data acquired at a frequency of 10 Hz. Simultaneously, continuous video footage of the panel and ballast was acquired from directly above the leading end of the test arrangement shown in Fig. 3. The ballast was re-prepared between each test repeat to ensure a consistent ballast density, formation, and distribution.

3 Results

The sections below present the results of tests 1–42 (as summarised in Table 2). Each result is presented as the average of the three repeats completed at each spacing, which better represents the aggregate behaviour of a bulk track system. A numerical summary of each test is shown in Table 3. The characterising lateral resistance values presented are displacements at 3 mm, 10/15 mm (which is an average of the lateral resistance values found at this interval, for simplicity here-in referred to as ε), and also the peak value of lateral resistance. These are chosen as the early behaviour that is key in determining track buckling response as evaluated by a number of existing studies focussing on single sleeper characterisation [20, 46, 47], a modified bulk behaviour descriptor adapted from BS500:2000 [25] which describes behaviour at lateral displacements that correspond to horizontal track alignment values considered critical for mainline operation [48], and the maximum value reached during

Table 2 Test program and sleeper specification summary

Test No.	Ballast condition	Bed condition	Sleeper spacing (mm)	Sleeper type	Sleeper specification		
					Dimensions*	Mass per sleeper (kg)	Panel Mass, including rail (kg)
1–3	C	F	550	Concrete (G44)		299	1149
4–6			600				
7–9			650				
10–12			700				
13–15			750				
16–18			800				
19–21			850				
22–24	C	F	550	Steel (W560H)		93	531
25–27			600				
28–30			650				
31–33			700				
34–36			750				
37–39			800				
40–42			850				

*denotes dimensions not to scale, C = consolidated, and F = full

the test, respectively. The target lateral displacement for each test was 40 mm as this is the approximate maximum distance at which horizontal track alignment becomes (in the UK) a critical fault across a range of operating conditions [48].

The standard deviation (SD) of the lateral resistance value at each discrete displacement is also reported. Considering the total lateral resistance values only, tests undertaken with steel sleepers (SD range between 1.25 and 9.42) exhibit greater SD than those undertaken with concrete sleepers (SD range between 0.27 and 4.02). The SD of lateral resistance per sleeper (kN/m) values are of similar magnitude to those generated in existing SSPT literature (where reported) [23]. This indicates good repeatability between this research and existing literature, and that there is strong repeatability between sleeper type. Additionally, the maximum and minimum SD values occur at different sleeper spacings for both sleeper types suggesting that variation in lateral resistance values is the result of natural sleeper–ballast interaction not systematic error arising from test procedures.

3.1 Force–displacement plots

Lateral resistance values for all tests can be seen in Fig. 4, where the solid lines represent concrete (G44) sleepers and dashed lines represent steel (W560H) sleepers, presented as a traditional force–displacement plot. Although this type of presentation is uncommon in MSPT literature, it is useful for identifying that both sleeper types exhibit similar behaviour in the very small displacement region (shown in Fig. 4 inset) but that steel sleepers nearly always exceed the lateral resistance of concrete sleepers; except when compared to very narrow or very large spacings. However, Fig. 4 shows that steel sleepers begin to exhibit more effective lateral resistance behaviour at displacement values exceeding 3 mm. The values recorded at ε (highlighted in Fig. 4 as a region of interest) indicate that there is a non-linear correlation between lateral resistance and sleeper spacing for both steel and concrete sleepers, discussed further in Sect. 4. Under this assessment metric (kN), at ε, 700 mm is seen to be an optimum point for steel sleepers with respect to lateral resistance with 600 mm, 650 mm, and 800 mm very close below this. The results generated at 750 mm appear to be slightly lower than expected, but the extreme spacings of 550 mm and 850 mm are lower with respect to lateral resistance as excepted. Similarly, at ε, 650 mm is seen to the optimum point for concrete sleepers under these test conditions, with a very tight clustering of other spacings below this. The results generated at 800 mm are slightly lower than expected, but the general trend of more extreme spacings exhibiting lower values of lateral resistance remains true. The reasons for this behaviour are explored further in Sect. 3.2.

Lateral resistance values for all tests can again be seen in Fig. 5, where the solid lines represent G44 sleepers and dashed lines represent W560H sleepers, presented a traditional force–displacement plot with force normalised to the number of sleepers used, in this instance three. As noted in Table 1, this is the most common method of presenting TPPT results as it allows easy comparison to SSPT studies, whilst also capturing the overall behaviour of a number of sleepers. Interestingly, the values recorded at

Table 3 Lateral resistance values at a given displacement for tested sleepers, presented as an average of the three repeats completed under each condition (noted in Table 2)

Test No.	Sleeper type	Lateral resistance (kN)			Lateral resistance per sleeper (kN/sleeper)			Lateral resistance per metre (kN/m)		
		3 mm	ε	Peak	3 mm	ε	Peak	3 mm	ε	Peak
1–3	Concrete (G44)	18.07 ± 2.27	19.95 ± 1.92	24.63 ± 1.44	6.02 ± 0.76	6.65 ± 0.64	8.21 ± 0.48	10.95 ± 1.37	12.09 ± 1.17	14.93 ± 0.87
4–6		21.12 ± 2.63	22.47 ± 2.43	23.59 ± 1.31	7.04 ± 0.88	7.49 ± 0.81	7.86 ± 0.44	11.73 ± 1.46	12.48 ± 1.35	13.10 ± 0.73
7–9		21.46 ± 4.02	24.29 ± 3.60	29.00 ± 3.95	7.15 ± 1.34	8.10 ± 1.20	9.67 ± 1.32	11.00 ± 2.06	12.46 ± 1.85	14.87 ± 2.03
10–12		20.63 ± 1.70	23.33 ± 1.55	25.01 ± 1.09	6.88 ± 0.57	7.78 ± 0.52	8.34 ± 0.36	9.82 ± 0.81	11.11 ± 0.74	11.91 ± 0.52
13–15		20.01 ± 0.27	21.88 ± 1.47	23.95 ± 3.86	6.67 ± 0.09	7.29 ± 0.49	7.98 ± 1.29	8.90 ± 0.12	9.72 ± 0.65	10.65 ± 1.72
16–18		14.74 ± 0.55	16.82 ± 0.92	19.37 ± 0.91	4.91 ± 2.32	5.61 ± 2.68	6.46 ± 3.10	6.14 ± 2.90	7.01 ± 3.34	8.07 ± 3.88
19–21		18.56 ± 1.27	22.48 ± 1.36	26.94 ± 1.96	6.19 ± 0.42	7.49 ± 0.45	8.98 ± 0.65	7.28 ± 0.50	8.82 ± 0.53	10.56 ± 0.77
22–24	Steel (W560H)	21.48 ± 7.65	31.23 ± 9.42	41.28 ± 8.18*	7.16 ± 2.55	10.41 ± 3.14	13.76 ± 2.73*	13.02 ± 4.63	18.92 ± 5.71	25.02 ± 4.96*
25–27		25.54 ± 2.53	41.46 ± 4.66	70.87 ± 5.22*	8.51 ± 0.84	13.82 ± 1.55	23.62 ± 1.74*	14.19 ± 1.41	23.03 ± 2.59	39.37 ± 2.90*
28–30		28.35 ± 2.63	42.87 ± 4.05	50.78 ± 4.21*	9.45 ± 0.88	14.29 ± 1.35	16.93 ± 1.40*	14.54 ± 1.35	21.99 ± 2.08	26.04 ± 2.16*
31–33		31.43 ± 5.00	46.80 ± 3.15	75.89 ± 1.66*	10.48 ± 1.67	15.60 ± 1.05	25.30 ± 0.55*	14.97 ± 2.38	22.29 ± 1.50	36.14 ± 0.79*
34–36		25.94 ± 5.72	37.72 ± 5.36	48.18 ± 1.25*	8.65 ± 1.91	12.57 ± 1.79	16.06 ± 0.42*	11.53 ± 2.54	16.76 ± 2.38	21.41 ± 0.55*
37–39		28.25 ± 1.91	42.26 ± 4.35	71.52 ± 5.05*	9.42 ± 0.64	14.09 ± 1.45	23.84 ± 1.68*	11.77 ± 0.79	17.61 ± 1.81	29.80 ± 2.10*
40–42		22.45 ± 6.16	35.25 ± 7.64	49.85 ± 3.66*	7.47 ± 2.05	11.75 ± 2.55	16.62 ± 1.22*	8.79 ± 2.42	13.82 ± 2.99	19.55 ± 1.44*

*denotes test stopped before 40-mm displacement

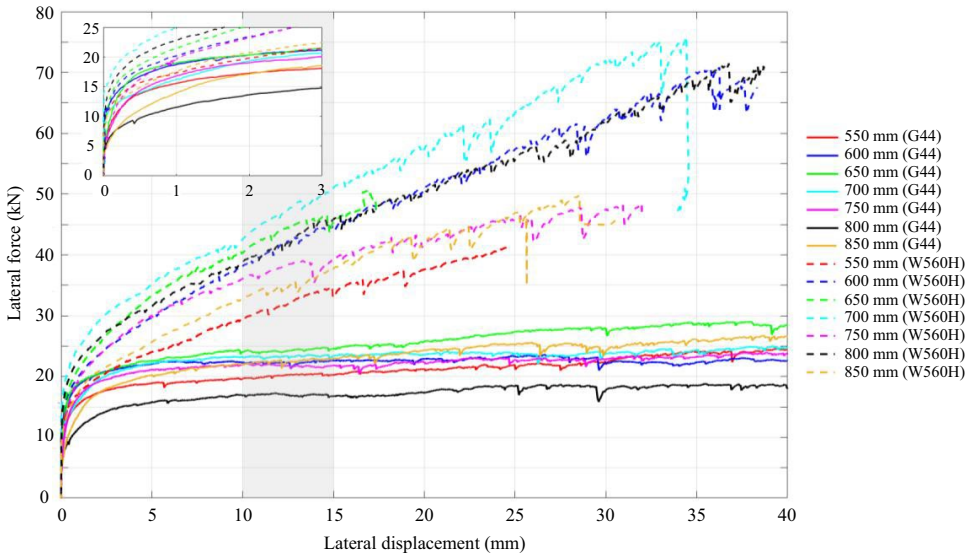

Fig. 4 Concrete (G44) and steel (W560H), force–displacement plot at different spacing conditions, presented as an average of the three repeats completed under each condition (inset: lateral displacement limited to 3 mm)

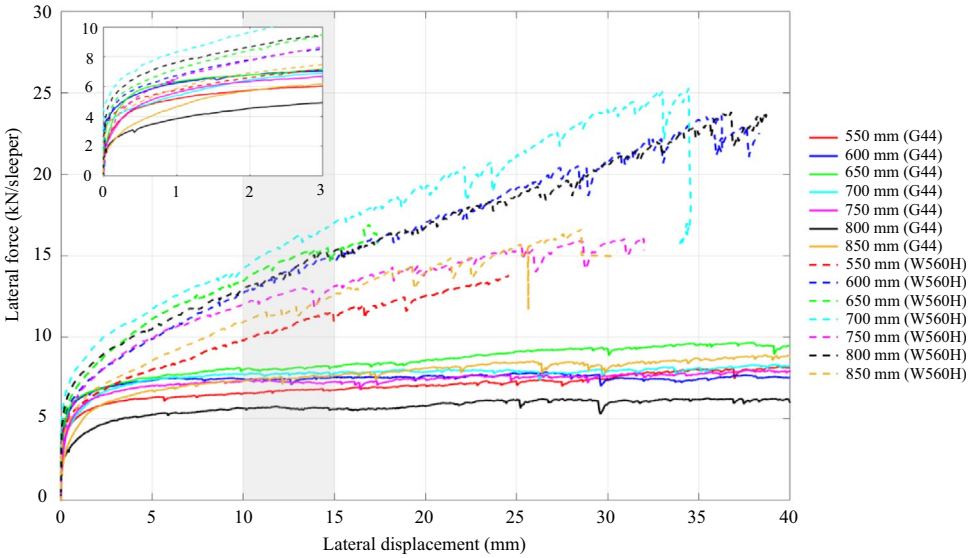

Fig. 5 Concrete (G44) and steel (W560H), force per sleeper–displacement plot at different spacing conditions, presented as an average of the three repeats completed under each condition (inset: lateral displacement limited to 3 mm)

the ε displacement, with a 600 mm sleeper spacing, for the G44 concrete sleeper are broadly comparable to the peak lateral resistance values generated from tests conducted in field conditions (i.e. using dynamic track stabilisation and full size tamping equipment) as reported by other authors including Pucillo et al. [37, 38] and De Iorio et al. [36]. The majority of these values were found at similar displacements, which would suggest that the consolidation levels during the tests completed in this study were at least comparable to those generated on track. Given that this is a simple normalisation, under this assessment metric (kN/sleeper), the relative performance of each sleeper spacing with respect to lateral resistance remains the same as that shown in Fig. 4 (albeit with lateral resistance values three times smaller), including at very small displacements. The reasons for this behaviour are explored further in Sect. 3.2.

Normalising lateral force by track length rather than by sleeper, Fig. 6 uses solid lines to represent G44 sleepers and dashed lines represent W560H sleepers. Given the clear influence of spacing on sleeper lateral resistance, noted in Figs. 4 and 5, this should be the most effective method of understanding the direct effect of spacing on

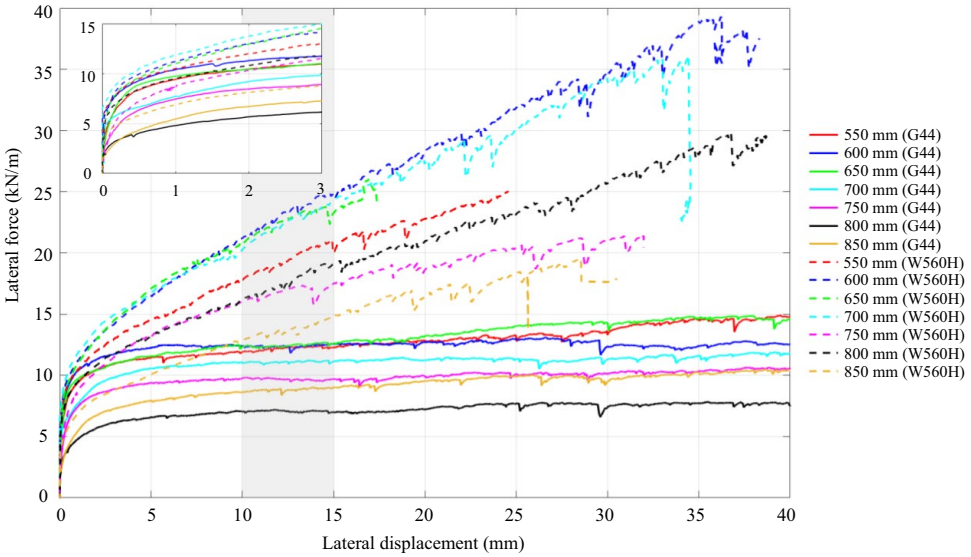

Fig. 6 Concrete (G44) and steel (W560H), force per metre–displacement plot at different spacing conditions, presented as an average of the three repeats completed under each condition (inset: lateral displacement limited to 3 mm)

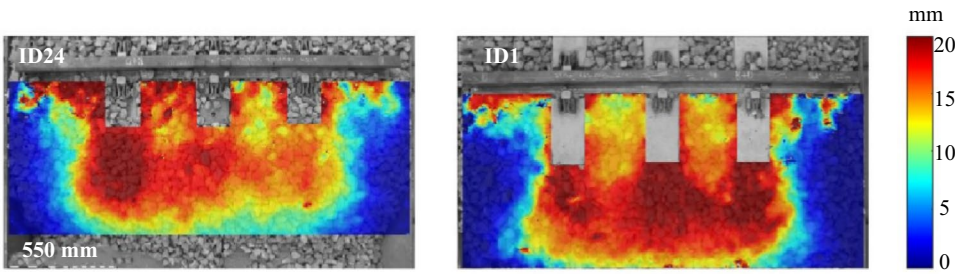

Fig. 7 Digital image correlation analysis for steel (ID24, 22.81 kN/m) and concrete (ID1, 12.83 kN/m) lateral resistance test at 550 mm spacing, limited to 20-mm lateral displacement

lateral resistance. Using this assessment metric (kN/m), clear differences between each spacing begin to emerge (explored further in Sect. 4). This time, at ε, 600 to 700 mm are clear optimum points with respect to lateral resistance for steel sleepers under these test conditions with near identical force responses across the displacement distance. Interestingly, 550 mm becomes greater with respect to lateral resistance than the other three remaining spacings with 850 mm being the lowest. Similarly, 550–650 mm are clear optimum points with respect to lateral resistance for concrete sleepers under there test conditions. The lateral resistance values of spacings between 700 and 850 mm are significantly lower at this point. Likewise, the behaviour of both sleepers at very small displacements (Fig. 6 inset) is very different, with concrete exhibiting similar behaviour to steel sleepers in some cases (e.g. at 600 mm). The reasons for this behaviour are explored further in Sect. 3.2

3.2 Digital image correlation

The data presented in Sect. 3.1 show sleeper spacing has a significant influence on lateral resistance values, with a non-linear relationship noted between the two for both sleeper types. Utilising novel digital image correlation (DIC) techniques, described in Sect. 2, the mechanisms behind this behaviour can be inferred through surface level ballast movement analysis. Figures 7–13 show ballast movement in the region ahead of the leading edge of three sleepers, referred to here-in as the ballast propagation zone, representing the area through which stresses and displacements induced by sleeper movement are transmitted through the ballast. These are shown for a given test at a spacing for both steel (left) and concrete (right), where the analysis is limited to the region of interest (as noted in Sect. 3 this is below 20 mm of displacement). In this instance, dark blue indicates zero (or near zero) movement, whereas dark red indicates up to 20 mm of movement at the surface. The average lateral resistance (kN/m) generated at this displacement is noted for

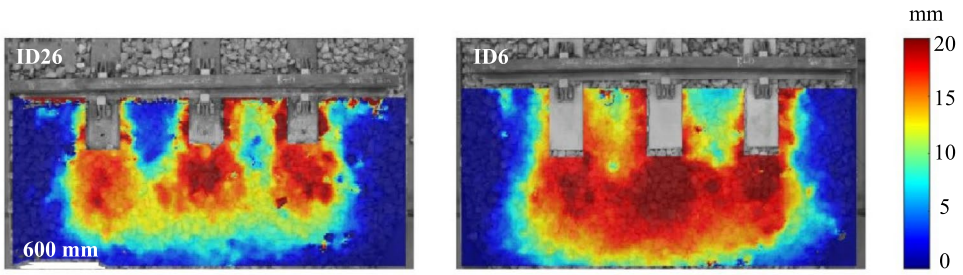

Fig. 8 Digital image correlation analysis for steel (ID26, 28.36 kN/m) and concrete (ID6, 12.71 kN/m) lateral resistance test at 600 mm spacing, limited to 20-mm lateral displacement

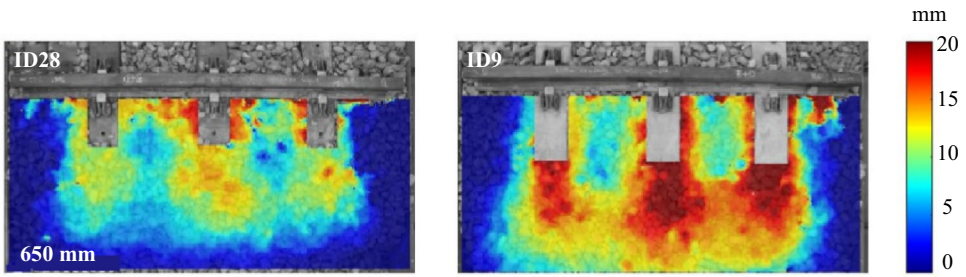

Fig. 9 Digital image correlation analysis for steel (ID28, 25.19 kN/m) and concrete (ID9, 13.22 kN/m) lateral resistance test at 650 mm spacing, limited to 20-mm lateral displacement (note that steel sleeper tests at 650-mm were completed to a restricted displacement)

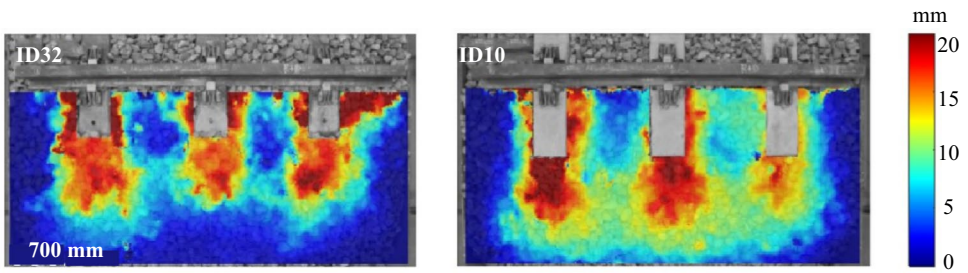

Fig. 10 Digital image correlation analysis for steel (ID32, 27.38 kN/m) and concrete (ID10, 11.22 kN/m) lateral resistance test at 700-mm spacing, limited to 20 mm lateral displacement

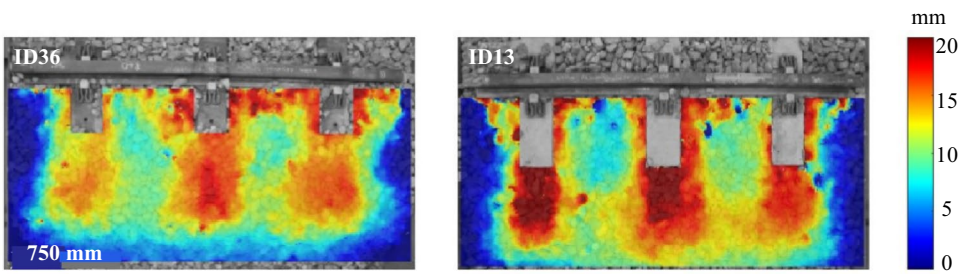

Fig. 11 Digital image correlation analysis for steel (ID36, 18.62 kN/m) and concrete (ID13, 9.93 kN/m) lateral resistance test at 750-mm spacing, limited to 20 mm lateral displacement

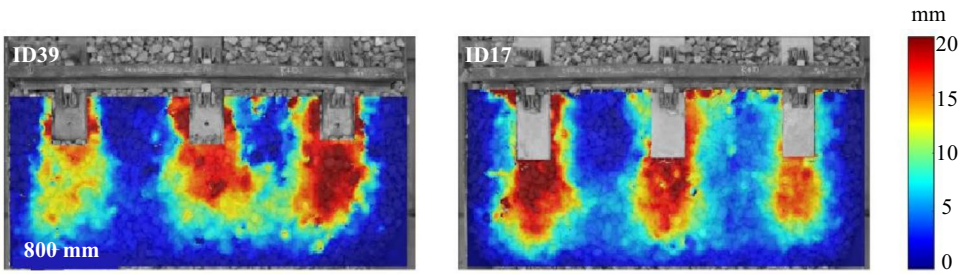

Fig. 12 Digital image correlation analysis for steel (ID39, 20.93 kN/m) and concrete (ID17, 7.23 kN/m) lateral resistance test at 800-mm spacing, limited to 20 mm lateral displacement

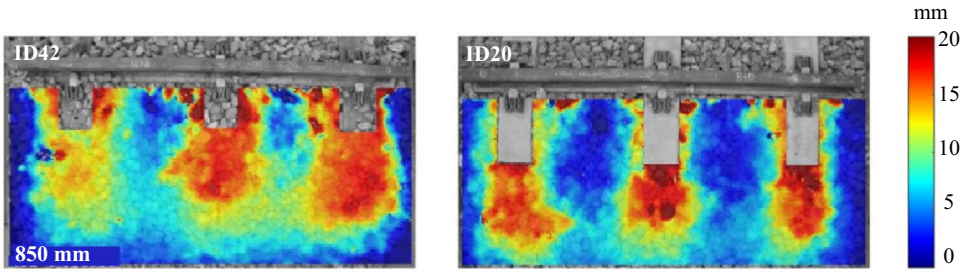

Fig. 13 Digital image correlation analysis for steel (ID42, 16.46 kN/m) and concrete (ID20, 9.55 kN/m) lateral resistance test at 850-mm spacing, limited to 20 mm lateral displacement

each image. It should be noted that the comparisons drawn throughout this section are qualitative only: The DIC system used here is designed to capture broad surface displacement patterns rather than resolve individual particle trajectories or calculate volumetric ballast flow. As such, a quantitative comparison between images is not required.

In general, the DIC observations reveal distinct differences between steel and concrete sleepers. Steel sleepers produce narrow, consistent propagation zones originating near the sleeper spades, suggesting that vertical stress transmission dominates their interaction with the ballast. In contrast, concrete sleepers generate broader, cone-shaped propagation zones, indicating more distributed lateral stress paths and engagement of a larger volume of surrounding ballast. This is explored further below.

Figure 7 shows the typical ballast movement ahead of steel (ID24) and concrete (ID1) sleepers at 550 mm spacing. In this instance, it can be seen that similar amounts of ballast material are displaced, with significant interference between each propagated ballast zone (seen here as the projection of a cone). There is a difference in the shape of the ballast propagation zone ahead of each sleeper type. The concrete sleepers generate a zone of movement which propagates neatly from the sleeper end into a cone projection multiple times wider at the largest end. In contrast, the steel sleepers produce a much narrower overall zone that stays approximately consistent in size across its distance but propagates from outside the visible sleeper end. This distance is approximately that of the sub-surface sleeper spades suggesting that this causes additional surface movement through lines of vertical ballast propagation (explored further in Sect. 4). The analysis indicates that in both cases a significant volume of ballast is mobilised as a result of sleeper movement at this narrow separation distance, in a motion that can be described as 'bulk' movement, with additional inter-sleeper ballast mobilised when compared to extended spacings (as seen in Figs. 11, 12, 13).

Figure 8 shows the typical ballast movement ahead of steel (ID26) and concrete (ID6) sleepers at 600 mm spacing. In comparison with Fig. 7, there is a reduced amount of ballast mobilisation present in the case of the steel sleeper with clear inter-sleeper–ballast interaction, whereas the concrete sleeper appears to behave similarly to the narrower spacing. This difference in behaviour is indicative of the difference in the zone of ballast propagation between both sleeper types. This explains the very similar lateral resistance values generated by the concrete sleeper at these spacings. However, despite the reduced volume of ballast mobilisation the steel sleeper lateral resistance value generated here is the optimum point when normalised by spacing. This would suggest that at this spacing the ballast movement acts constructively within the 'zone of influence' to increase overall resistance to movement, as noted in Fig. 1. Although this analysis is only at a surface level, it is likely that this interference also occurs sub-surface to accentuate and enhance this effect. In this instance, non-uniform panel behaviour can be seen

ID24, in which the left-most sleeper has displaced more than the right-most one. Although this does not affect the numerical outcome of the test, it does indicate how sensitive lateral behaviour of railway track is to longitudinal alignment.

Figure 9 shows the typical ballast movement ahead of steel (ID28) and concrete (ID9) sleepers at 650 mm spacing. As noted in Table 3, the lateral resistance values generated by both sleeper types are very similar at 600 as it is at 650 mm, particularly when normalised by sleeper spacing. Congruently, this is reflected in the similarity between Figs. 8 and 9. Although the increase in spacing distance means that the amount of ballast volume moved at the surface has decreased, it is clear that the ballast propagation from the end of each sleeper is constructively interfering within the 'zone of influence' to maintain overall lateral resistance.

Figure 10 shows the typical ballast movement ahead of the steel (ID32) and concrete (ID10) sleepers at 700 mm spacing. Again, as noted in Table 3, the lateral resistance values generated by both sleeper types are very similar at 700 mm as it is at 600 and 650 mm; albeit reducing in the case of the concrete sleeper. However, this behaviour is clearly directly related to the surface ballast behaviour exhibited. The steel sleeper–ballast movement is very similar to that shown in Fig. 9, but with distinct regions of movement ahead of each sleeper beginning to appear which result in reduced inter-sleeper interaction. This is expected behaviour given the noted propagated ballast zone geometry and, when taken with the lateral resistance behaviour, suggests that, in the case of the steel sleeper, it is indeed sub-surface ballast interaction inside, around, and ahead of the sleeper that is generating much of the lateral resistance performance. The concrete sleeper behaviour is also to be expected, as the greater sleeper spacing leads to ballast propagation zones which are gradually reducing in interaction thus reducing overall lateral resistance performance.

Figure 11 shows the typical ballast movement ahead of steel (ID36) and concrete (ID13) sleepers at 750 mm spacing. As shown in Fig. 7 and Table 1, 750 mm is the point at which the lateral resistance values of both sleeper types begin to significantly decrease, with similar but a definite reduction in inter-sleeper interaction visible. Although this is not as clear when compared to larger spacings (Figs. 12 and 13), it is evident that this is the point at which the small amount of surface interaction ceases to translate into sub-surface constructive interference between each sleeper.

Figure 12 shows the typical ballast movement ahead of steel (ID39) and concrete (ID17) sleepers at 800 mm spacing. As previously noted, it is clear that at 800 mm and 850 mm (Fig. 13), which are very wide spacings, almost all inter-sleeper–ballast interaction ceases. This leaves visible pockets of undisturbed surface level ballast. The reduction in lateral resistance at these spacings would suggest that this interaction is also significantly reduced at the sub-surface level, with any differences in lateral resistance value attributed to overall ballast bed consolidation which is difficult to control absolutely under laboratory conditions.

Figure 13 shows the typical ballast movement ahead of steel (ID42) and concrete (ID20) sleepers at 850 mm spacing. The ballast movement at this spacing is very similar to that shown in Fig. 12, which is to be expected. As noted, it can be inferred that the slight rise in lateral resistance values at this spacing are down to a more consolidated ballast bed, particularly in the concrete tests. This can be seen in a more uniform ballast movement distribution ahead of each sleeper, compared to that shown in Fig. 12.

While DIC captures only surface displacements, these patterns provide mechanistic insight into sub-surface ballast behaviour. The narrow steel propagation zones suggest a concentrated transfer of loads through vertical ballast propagation, whereas the broader concrete zones indicate a wider ballast mobilisation regime. However, it should be noted that 3D ballast interactions and particle interlocking are not directly observed and may influence actual sub-surface behaviour. Overall, the DIC analysis supports the interpretation that the non-linear relationship between sleeper spacing, and lateral resistance arises from the constructive or diminishing interference of ballast movement between sleepers, with both surface and inferred sub-surface mechanisms contributing to the observed behaviour.

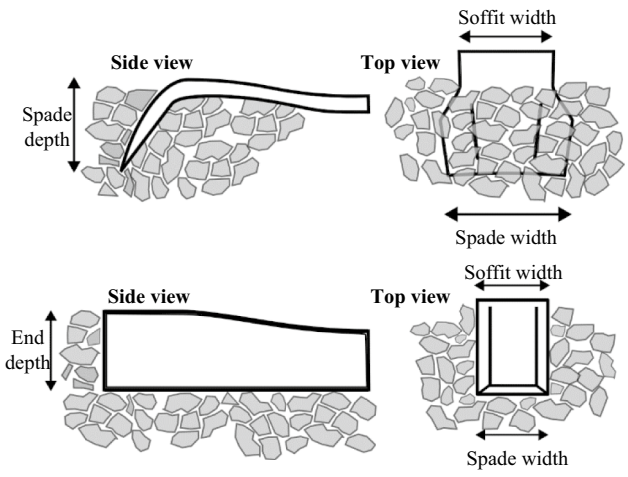

Fig. 14 Steel (W560H) (top) and concrete (G44) (bottom), sleeper–ballast interaction with respect to geometry

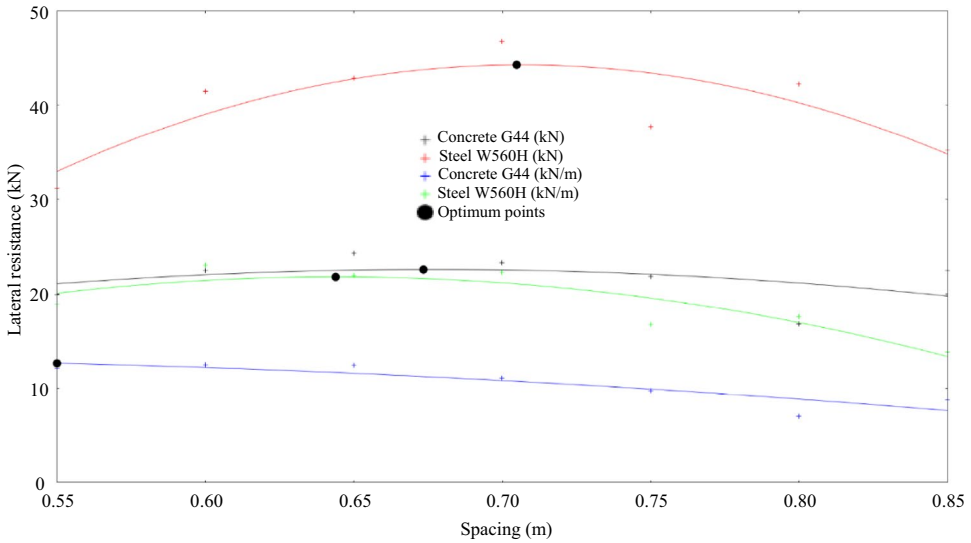

Fig. 15 Concrete (G44) and steel (W560H), lateral resistance performance at the ε point at different sleeper spacings presented as overall lateral resistance and lateral resistance normalised by sleeper spacing

4 Discussion

To better understand the effect of sleeper spacing the performance of both concrete and steel sleepers, the lateral resistance behaviour has been examined under seven distinct sleeper spacings utilising a novel MSPT methodology which limits the uplift displacement a sleeper panel can experience during a test whilst allowing for up to three sleepers to be tested in combination. This unique test apparatus means that these tests can be completed to lateral displacements much greater than most existing literature, whilst monitoring surface level ballast movement to gain a deeper insight into sleeper behaviour under the given conditions. However, some tests within this study were limited in lateral displacement as a result of force limitations associated with some elements of the experimental apparatus, although this did not affect outcomes of the study. Where it is possible to compare lateral resistance values to existing literature, the values are within a maximum of 12% of those reported for both laboratory and field experiments. However, as is expected, all values were lower than those found during experiments which reported the use of dynamic track stabilisation techniques. Although this highlights how difficult it is to replicate real world consolidation techniques within a laboratory setting, the lateral resistance values generated were within one SD. This suggests that the level of consolidation reached within this study is a reasonable approximation for that found within the real track system or, at least, that the relatively unique three sleeper experimental set-up is able to mimic real track system responses through close replication of the real track system. When taken together, these two factors strongly suggest that the relative ranking of results would be the same as if a real track system had been used to conduct the tests.

As described in Sect. 3, the differences in lateral resistance behaviour between each sleeper type—particularly at distances beyond 5 mm—suggest that sub-surface sleeper–ballast interaction has a critical role in governing overall lateral resistance (i.e. behaviour not immediately evident in the surface level analysis shown in Figs. 7–13). Although several mechanisms may contribute to this, the most likely explanation relates to differences in sleeper geometry, both internal and external, as shown in Fig. 14.

The surface DIC analysis provides a comprehensive view of how surface movement occurs, but also indirectly indicates how ballast may be mobilised beneath the surface because, as discussed in Sect. 3, each sleeper type displays unique surface propagation behaviour. As can be seen, in the case of the steel sleeper, the spade (which constitutes the sleeper end) is embedded within the ballast due to the concave soffit geometry. Furthermore, the spade end is significantly wider than the central sleeper soffit. This geometry produces a wider engagement zone at the sleeper ends, which likely promotes deeper and more laterally distributed ballast mobilisation, aligning with the broader and more dispersed propagation zone patterns observed in Sect. 3. In contrast, the concrete sleeper only interacts with ballast directly ahead of its geometrical boundaries—explaining why ballast movement propagates directly from this region with very little deviation.

Previous studies have shown that steel sleepers generate more of their overall lateral resistance from internal sleeper–ballast interactions than concrete sleepers, and due to their shape invoke additional contributions from

Table 4 Summarised peak lateral resistance at ε values and associated optimum sleeper spacing for steel (W560H) and concrete (G44) utilising different lateral resistance assessment metrics

Sleeper type	Lateral resistance assessment metric	Peak lateral resistance at ε	Optimum sleeper spacing (mm)
Steel (W560H)	Overall (kN)	44.27	706
	Normalised (kN/m)	22.05	643
Concrete (G44)	Overall (kN)	22.59	675
	Normalised (kN/m)	12.66	550

pseudo-crib and pseudo-end contributions [23], which supports the inferences made about the relationship between surface and sub-surface behaviour. Although caution should be taken when applying this inference, the consistency between sleeper geometry, observed DIC patterns, and the corresponding lateral resistance trends provides a coherent mechanistic explanation linking surface and sub-surface behaviour.

The results presented in Figs. 4, 5 and 6 show that there is a difference between assessing lateral resistance performance and behaviour as a whole panel of a given number of sleepers (kN), normalised for the number of sleepers present (kN/sleeper), or normalised for the sleeper spacing used (kN/m). Although conventional SSPTs only allow for an assessment of lateral resistance to make using the first two methods, an MSPT using the configuration described enables a spacing normalised assessment. This unlocks the ability to fairly compare the behaviour of sleepers at different spacings whilst also enabling the assessment of a system, which is vital for informing optimised track system design. This is highlighted by the summarised results, shown in Fig. 15, which presents both overall lateral resistance and lateral resistance normalised by sleeper spacing at the ε value against sleeper spacing.

Utilising this discretised description of lateral resistance behaviour, lateral resistance values can be directly related to sleeper spacing and an optimum point found under each condition. In each instance, the function is formed to avoid mutual dependency between each parameter to ensure that the function is able to converge sufficiently during fitting.

The following equations describe the fitted functions, ρ is lateral resistance:

Concrete G44 (kN)

$$\rho(s_\mathrm{d}) = -93.688(s_\mathrm{d} - 0.675)^2 + 0.355(s_\mathrm{d}) + 22.350, \quad (1)$$

Steel W560H (kN)

$$\rho(s_\mathrm{d}) = -459.885(s_\mathrm{d} - 0.706)^2 + 0.359(s_\mathrm{d}) + 44.021, \quad (2)$$

Concrete G44 (kN/m)

$$\rho(s_\mathrm{d}) = -30.710(s_\mathrm{d} - 0.550)^2 - 7.573(s_\mathrm{d}) + 16.825, \quad (3)$$

Steel W560H (kN/m)

$$\rho(s_\mathrm{d}) = -198.298(s_\mathrm{d} - 0.643)^2 + 0.1359(s_\mathrm{d}) + 21.819. \quad (4)$$

Applying the fitted functions described by Eq. (1)–(4) results in the derivation of the likely optimum sleeper spacing for each sleeper type as shown in Fig. 9 and summarised in Table 4.

These derivations show that when the system is conventionally assessed using overall lateral resistance, the optimum sleeper spacing for steel sleepers is approximately 706 mm whilst concrete sleepers have an optimum sleeper spacing of approximately 675 mm. These are both larger than the standard spacing of 650 mm used by many infrastructure operators (including the UK [6]). When considered in this way, as shown in Fig. 9, the concrete sleeper lateral resistance curve is notably flatter than that of steel sleepers, which suggests that the type is less sensitive to changes in spacing—behaviour which is consistent with the mechanisms described above. Although the overall lateral resistance of concrete sleepers is approximately half that of the steel sleeper, the flatter curve suggests that more similar, predictable behaviour could be expected across spacing variations.

Additionally, despite near complete ballast mobilisation, smaller spacings (e.g. 550 mm) for both sleeper types do not exhibit a significant increase in lateral resistance performance when compared to much wider spacings (e.g. 850 mm). This suggests that reducing sleeper spacing to increase lateral resistance performance of a track system will not necessarily be of benefit and could be detrimental to the overall system when assessed holistically (i.e. an additional financial and environmental cost is introduced). When considered as lateral resistance normalised by sleeper spacing, the optimum sleeper spacing, and corresponding peak lateral resistance value, reduce for both sleeper types. In this instance the steel sleeper value drops to approximately 643 mm, whilst the concrete sleeper value reduces significantly to approximately 550 mm, whilst the fitted curves are significantly flatter for both types. This means that smaller sleeper spacings are much similar in lateral resistance (or in the case of the concrete sleeper, the optimum) to the optimum point and are much greater than wider spacings (e.g. 850 mm)—this agrees with the image analysis described in Sect. 3.

However, although there is clear scope to increase track lateral stability through the optimisation of sleeper spacing and the selection of appropriate sleeper types, alterations to both do have broader implications for overall track behaviour

and performance which must be considered. A reduction in sleeper spacing increases overall track stiffness, which tends to elevate rail bending moments and vertical contact stresses thus accelerating material degradation and fatigue phenomena [6]. Conversely, wider spacing increases the unsupported span between rail support points which increases vertical rail deflections and thus bending moments, which can accelerate ballast breakdown and settlement [9]. Furthermore, the chosen sleeper type and loading on the system can also influence track performance. Sleepers which have a lower mass, like steel, can respond differently under dynamic train loads which can affect wheel–rail contact forces and overall track dynamic response [49]. This underscores the fact that decisions about the track system must be considered holistically, and not by single metrics. Ultimately this means that parameters such as sleeper spacing must be evaluated and optimised alongside other key parameters including lateral resistance, track stiffness, dynamic load distribution, rail specification, or maintenance demands to avoid unintended system degradation, safety risks, or other operational constraints (e.g. steel sleepers are generally not suitable for use in third-rail electrification areas due to electrical insulation and clearances [15]).

5 Conclusions

The characterisation of lateral resistance properties of railway sleepers in ballast track is vital in ensuring overall track stability, and the assessment of this property, and its associated parameters, is critical to overall track design and component selection. In the work presented, the influence of sleeper spacing on the lateral resistance performance of both concrete (G44) and steel (W560H) sleepers has been compared in a laboratory environment using a novel full-scale MSPT methodology, comprised of three sleepers. This is the first direct comparison between the behaviour of modern concrete and sleeper variants in this arrangement. The most important results are summarised as follows:

1. Steel sleepers outperform concrete sleepers, with respect to lateral resistance, at lateral displacements greater than 3 mm, while both perform similarly at small displacements.
2. The crossover displacement occurs below 10 mm, which is a shorter displacement when compared to SSPT observations—likely due to the conditions imposed upon the sleepers being more representative of those found in track.
3. Optimal sleeper spacing is approximately 706 mm for steel sleepers and 675 mm for concrete sleepers, when overall lateral resistance is considered.
4. Concrete sleepers exhibit a much flatter lateral resistance curve indicating lower sensitivity to spacing changes, whereas steel sleepers maintain higher resistance over a narrower spacing range.
5. Narrow sleeper spacings offer limited additional benefit, with respect to lateral resistance, suggesting potential unnecessary financial and environmental costs.

Overall, this work has shown that MSPTs have the potential to produce a more effective means of assessing and characterising both sleeper and track behaviour, particularly with respect to lateral resistance, when compared to SSPTs. This is because they better replicate in situ field conditions and allow the critical inter-sleeper–ballast interaction to occur. However, MSPTs are inherently more resource-intensive to undertake, requiring additional equipment and increased test durations and so may not always be the best method within a laboratory setting. Future studies should seek to expand the presented work to firstly include a wider range of sleeper types used in contemporary railway infrastructure and secondly examine the effects of ballast dimensions on lateral resistance during MSPTs (particularly related to the ballast shoulder). Additionally, an opportunity now exists to examine the broader, system-level implications of altering sleeper spacing beyond lateral resistance performance (i.e. overall environmental impacts, or wheel–rail contact performance) through data-driven insights derived from unique datasets. The examination of these effects could inform more efficient spacing strategies (i.e. safely increase the separation distance between each sleeper without a reduction in system performance), ultimately reducing embedded carbon and infrastructure costs through a change in established infrastructure design practices whilst helping support the transition to lower carbon transport networks and increasing network resilience.

Acknowledgements The authors would like to thank Dr Andy Trowsdale and Scott Dyball for their assistance in completing this work. The authors would also like to thank Dr Iwo Słodczyk and Nigel Shaw for their technical insights. The authors would like to thank the Engineering and Physical Sciences Research Council (EPSRC) through the Advanced Metallic Systems Centre for Doctoral Training (EPSRC grant ref. EP/S022635/1) and British Steel Limited for providing the funding for this research.

Data availability Data supporting this publication can be freely downloaded from the University of Sheffield research data repository at https://doi.org/10.15131/shef.data.26476000.v1 and https://doi.org/10.15131/shef.data.28904618.v1 under the terms of the Creative Commons Attribution (CC BY) licence.

References

1. Iwnicki S (2006) Handbook of railway vehicle dynamics, 1st edn. CRC Press, Boca Raton
2. Zhao J, Chan AC, Burrow MN (2007) Reliability analysis and maintenance decision for railway sleepers using track condition information. J Oper Res Soc 58(8):1047–1055
3. Liu J, Du S, Liu G et al (2023) Influence of unsupported sleepers on the dynamic stability of ballasted bed based on wheelset impact tests. Railw Eng Sci 31(1):52–60
4. Kish A, Samavedam G (1991) Dynamic buckling of continuous welded rail track: theory, tests, and safety concepts. In: Conference on lateral track stability. St Louis, No. 1289, Transportation Research Record.
5. Ellis I (2001) Track terminology (British Railway Track). Permanent Way Institution, Ingatestone
6. Sañudo R, Miranda M, Alonso B et al (2022) Sleepers spacing analysis in railway track infrastructure. Infrastructures 7(6):83
7. Koyama E, Ito K, Hayano k et al (2021) A new approach for evaluating lateral resistance of railway ballast associated with extended sleeper spacing. Soils Found 61(6):1565–1580
8. Sutar A, Tande S (2024) Effect of H-beam and double channel sleeper spacing and positioning on steel girder railway bridge using FEM. Innov Infrastruct Sol 9(12):479
9. Sañudo Ortega R, Pombo J et al (2021) The importance of sleepers spacing in railways. Constr Build Mater 300:124326
10. Bogacz R, Czyczuła W, Konowrocki R (2014) Influence of sleepers shape and configuration on track-train dynamics. Shock Vib 2014:393867
11. Grassie SL (2009) Rail corrugation: characteristics, causes, and treatments. Proceed Inst Mech Eng, Part F: J Rail Rapid Transit 223(6):581–596
12. Schmid F (2010) Best practice in wheel–rail interface management for mixed traffic railways, 1st edn. University of Birmingham Press, Birmingham
13. Hasan N (2015) Railroad tie spacing related to wheel-load distribution and ballast pressure. Pract Period Struct Des Constr 20(4):04014047
14. Wu T, Thompson DJ (2000) The influence of random sleeper spacing and ballast stiffness on the vibration behaviour of railwaytrack. Acta Acust United Acust 86(2):313–321
15. Network Rail (2021) Design and construction of track, NR/L2/TRK/2102. London
16. Société Nationale des Chemins de Fer Français. SNCF 0221: Règles de conception de la voie ferrée. Paris
17. Deutsche Bahn (2021) Ril 800.0110: Planung von Oberbauarten. Berlin
18. Zhao W, Xiao H, Li X (2025) Mechanical behavior analysis of enhanced railway sleepers for small radius curves. Comput Part Mech 12(5):2745–2758
19. Sañudo R, Cerrada M, Alonso B et al (2017) Analysis of the influence of support positions in transition zones. A numerical analysis. Constr Build Mater 145:207–217
20. Słodczyk I, Whittle J, Fletcher D et al (2025) Improved lateral resistance test: investigating the effect of a partial uplift restraint during a single sleeper push test. Transp Res Rec 2679(4):554–569
21. Whittle JW, Danks S, Słodczyk I et al (2024) Using digital image correlation (DIC) to measure railway ballast movement in full-scale laboratory testing of sleeper lateral resistance. Proceed Inst Mech Eng, Part F: J Rail Rapid Transit 238(8):1037–1041
22. Chi Y, Xiao H, Wang Y et al (2024) Experimental study and numerical simulation of the impact of under-sleeper pads on the dynamic and static mechanical behavior of heavy-haul railway ballast track. Railw Eng Sci 32(3):384–400
23. Whittle JW, Słodczyk IA, Danks S et al (2025) Investigating the effect of railway track ballast and bed conditions on the lateral resistance of timber, concrete, steel, and composite sleepers using a novel test methodology. Eng Struct 340:120769
24. Koike Y, Nakamura T, Hayano K et al (2014) Numerical method for evaluating the lateral resistance of sleepers in ballasted tracks. Soils Found 54(3):502–514
25. British Standards Institution (2000) Steel sleepers, BS 500:2000. London
26. British Steel Limited (2016) Steel sleepers—installation guide. Scunthorpe
27. Sussmann T, Kish A, Trosino M (2003) Influence of track maintenance on lateral resistance of concrete-tie track. Transp Res Rec 1825(1):56–63
28. Bian X, Cai W, Luo Z et al (2023) Image-aided analysis of ballast particle movement along a high-speed railway. Engineering 27:161–177
29. Wang L, Meguid M, Mitri HS (2021) Impact of ballast fouling on the mechanical properties of railway ballast: insights from discrete element analysis. Processes 9(8):1331
30. Ngamkhanong C, Kaewunruen S, Baniotopoulos C (2021) Influences of ballast degradation on railway track buckling[J. Eng Fail Anal 122:105252
31. Chi Y, Xiao H, Zhang Z et al (2024) Influence of wind-blown sand content on the mechanical quality state of ballast bed in sandy railways. Railw Eng Sci 32(4):533–550
32. Xu C, Ito K, Hayano K et al (2023) Combined effect of supported and unsupported sleepers on lateral ballast resistance in ballasted railway track. Transp Geotech 38:100913
33. Le Pen LM, Powrie W (2011) Contribution of base, crib, and shoulder ballast to the lateral sliding resistance of railway track: a geotechnical perspective. Proc Inst Mech Eng Part F J Rail Rapid Transit 225(2):113–128
34. De Iorio A, Grasso M, Penta F et al (2018) On the ballast–sleeper interaction in the longitudinal and lateral directions. Proc Inst Mech Eng Part F J Rail Rapid Transit 232(2):620–631
35. International Union of Railways (2019) Lateral track resistance (LTR). Paris
36. De Iorio A, Grasso M, Penta F et al (2014) Transverse strength of railway tracks: part 1. Planning and experimental setup. Frattura Integrità Strutt 8(30):478–485
37. Pucillo GP (2020) Thermal buckling in CWR tracks: critical aspects of experimental techniques for lateral track resistance evaluation. In: 2020 Joint Rail Conference. St. Louis, pp V001T08A009
38. Pucillo GP, Penta F, Catena M et al (2018) On the lateral stability of the sleeper-ballast system. Procedia Struct Integr 12:553–560
39. Reiner IA (1977) Lateral resistance of railroad track. FRA/ORD-77/41, United States Department of Transportation, Washington D.C.
40. Van't Zand J, Moraal J (1997) Ballast resistance under three dimensional loading. Dissertation, Delft University

41. McHenry M, LoPresti J (2016) Field evaluation of sleeper and fastener designs for freight operations. In: the 11th World Congress on Railway Research (WCRR2016), Milan, 29 May–2 June, 2016
42. US Federal Railroad Administration (2008) Evaluation of tie plate cracking on composite ties. RR08–21, Pueblo
43. Network Rail (2021) Track ballast and stoneblower aggregate. NR/L2/TRK/8100, London
44. British Steel Limited (2023) Development of a new lateral resistance test rig. 2023-I005, Scunthorpe
45. Whittle JW, Slodczyk I (2024) Lateral resistance testing and finding applications. In: British Steel Annual Technical Forum, Scunthorpe, 14 May 2024
46. Aela P, Jitsangiam P, Li X et al (2023) Influence of ballast bulk density and loading conditions on lateral resistance of concrete sleeper components. Proc Inst Mech Eng Part F J Rail Rapid Transit 237(10):1284–1293
47. Jing G, Fu H, Aela P (2018) Lateral displacement of different types of steel sleepers on ballasted track. Constr Build Mater 186:1268–1275
48. Network Rail (2023) Inspection & maintenance of permanent way: track geometry—inspections and minimum actions, NR/L2/TRK/001/mod11. London
49. Montalban L, Zamorano C, Morales S et al (2015) Study of the influence of sleepers' material on track dynamics through numerical simulations. J Vibroeng 17(7):3832–3843